

AD-A199 955

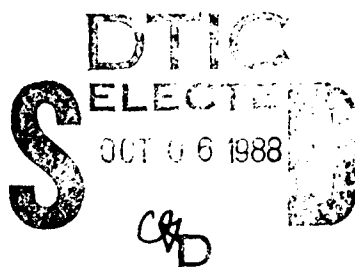
FILE COPY AFOSR-TR-88-0998

(2)

## TWO PHOTON DETECTION TECHNIQUES FOR ATOMIC FLUORINE

June 1988

Final Report



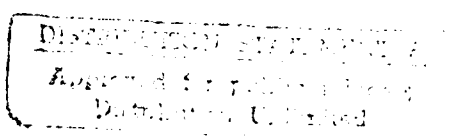
By: William K. Bischel

Prepared for:

AIR FORCE OFFICE OF SCIENTIFIC RESEARCH  
Building 410  
Bolling Air Force Base  
Washington, DC 20332-6448

Attention: Dr. Julian Tishkoff

SRI Project PYC-8320



SRI International  
333 Ravenswood Avenue  
Menlo Park, California 94025-3493  
(415) 326-6200  
TWX: 910-373-2046  
Telex: 334486



20 10 3 30

Unclassified

SECURITY CLASSIFICATION OF THIS PAGE

Form Approved  
OMB No. 0704-0188

## REPORT DOCUMENTATION PAGE

1a. REPORT SECURITY CLASSIFICATION Unclassified		1b. RESTRICTIVE MARKINGS													
2a. SECURITY CLASSIFICATION AUTHORITY		3. DISTRIBUTION/AVAILABILITY OF REPORT Approved for public release; distribution is unlimited.													
2b. DECLASSIFICATION/DOWNGRADING SCHEDULE		5. MONITORING ORGANIZATION REPORT NUMBER(S) <b>AFOSR-TK-88-0998</b>													
4. PERFORMING ORGANIZATION REPORT NUMBER(S)		7a. NAME OF MONITORING ORGANIZATION <b>AFOSR/NA</b>													
6a. NAME OF PERFORMING ORGANIZATION SRI International	6b. OFFICE SYMBOL (If applicable)	7b. ADDRESS (City, State, and ZIP Code) Building 410, Bolling AFB DC 20332-6448													
8a. NAME OF FUNDING/SPONSORING ORGANIZATION <b>AFOSR/NA</b>	8b. OFFICE SYMBOL (If applicable) <b>NA</b>	9. PROCUREMENT INSTRUMENT IDENTIFICATION NUMBER F49620-85-K-0005													
8c. ADDRESS (City, State, and ZIP Code) Building 410, Bolling AFB DC 20332-6448	10. SOURCE OF FUNDING NUMBERS <table border="1"><tr><td>PROGRAM ELEMENT NO. <b>61102F</b></td><td>PROJECT NO. <b>2308</b></td><td>TASK NO. <b>A3</b></td><td>WORK UNIT ACCESSION NO.</td></tr></table>			PROGRAM ELEMENT NO. <b>61102F</b>	PROJECT NO. <b>2308</b>	TASK NO. <b>A3</b>	WORK UNIT ACCESSION NO.								
PROGRAM ELEMENT NO. <b>61102F</b>	PROJECT NO. <b>2308</b>	TASK NO. <b>A3</b>	WORK UNIT ACCESSION NO.												
11. TITLE (Include Security Classification) <b>(U) TWO PHOTON DETECTION TECHNIQUES FOR ATOMIC FLUORINE</b>															
12. PERSONAL AUTHOR(S) W. K. Bischel															
13a. TYPE OF REPORT Final	13b. TIME COVERED FROM <u>850101</u> TO <u>880401</u>	14. DATE OF REPORT (Year, Month, Day) 880630	15. PAGE COUNT 42												
16. SUPPLEMENTARY NOTATION															
17. COSATI CODES <table border="1"><tr><th>FIELD</th><th>GROUP</th><th>SUB-GROUP</th></tr><tr><td></td><td></td><td></td></tr><tr><td></td><td></td><td></td></tr><tr><td></td><td></td><td></td></tr></table>	FIELD	GROUP	SUB-GROUP										18. SUBJECT TERMS (Continue on reverse if necessary and identify by block number) Multiphoton ionization spectroscopy, atomic fluorine.		
FIELD	GROUP	SUB-GROUP													
19. ABSTRACT (Continue on reverse if necessary and identify by block number) <p>This report describes research to develop a sensitive technique for the remote detection of atomic fluorine based on two-photon excitation of high-lying atomic states, followed by fluorescence. We report the first demonstration of two-photon excited laser induced fluorescence in F using a pump laser at 180 nm. In addition, we have also observed 3+2 resonantly-enhanced multiphoton ionization (REMPI) of F at 285 nm, and 3+1 REMPI of F at 233 nm. No fluorescence was observed for the three-photon excitation processes. We recommend directions for future research quantify this F-atom detection technique.</p>															
20. DISTRIBUTION/AVAILABILITY OF ABSTRACT <input checked="" type="checkbox"/> UNCLASSIFIED/UNLIMITED <input checked="" type="checkbox"/> SAME AS RPT <input type="checkbox"/> DTIC USERS	21. ABSTRACT SECURITY CLASSIFICATION Unclassified														
22a. NAME OF RESPONSIBLE INDIVIDUAL Julian M Tishkoff	22b. TELEPHONE (Include Area Code) <u>(202) 767-0465</u>	22c. OFFICE SYMBOL <b>AFOSR/NA</b>													

SRI International

RCS



## TWO PHOTON DETECTION TECHNIQUES FOR ATOMIC FLUORINE

June 1988

Final Report

By: William K. Bischel

Prepared for:

AIR FORCE OFFICE OF SCIENTIFIC RESEARCH  
Building 410  
Bolling Air Force Base  
Washington, DC 20332-6448

Attention: Dr. Julian Tishkoff

SRI Project PYC-8320

Approved by:

D. C. Lorents, Director  
Chemical Physics Laboratory

G. R. Abrahamson  
Vice President  
Physical Sciences Division

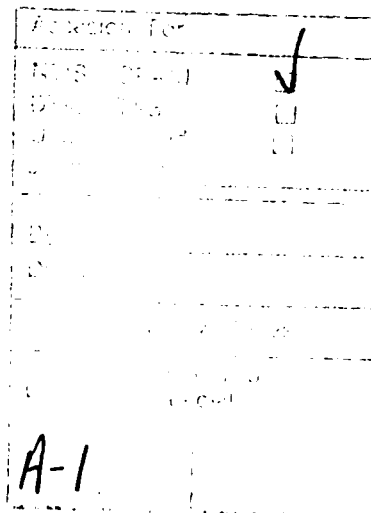
## CONTENTS

<b>ABSTRACT</b>	i
<b>INTRODUCTION</b>	1
<b>BACKGROUND</b>	3
Non-Laser Detection Techniques	3
Single-Photon Laser Detection Techniques	3
Two-Photon Excitation Methods	3
<b>SUMMARY OF RESEARCH ACCOMPLISHMENTS</b>	8
Two-Photon Detection of Atomic F	8
Three-Photon Resonantly Enhanced Multiphoton Ionization of F	12
Experiments Using Time-Of-Flight Mass Spectrometer	13
<b>CONCLUSIONS AND RECOMMENDATIONS</b>	15
<b>PUBLICATIONS AND CONFERENCE PRESENTATIONS</b>	17
<b>REFERENCES</b>	19
<b>APPENDICES</b>	

## Appendix A. TWO-PHOTON-EXCITED FLUORESCENCE SPECTROSCOPY OF ATOMIC FLUORINE AT 170 nm

## APPENDIX B. MULTIPHOTON IONIZATION SPECTROSCOPY OF ATOMIC FLUORINE

## APPENDIX C. MECHANISMS FOR $F^+$ PRODUCTION IN THE MULTIPHOTON IONIZATION OF $F_2$



## INTRODUCTION

Two-photon processes have been studied since the first pulsed ruby laser was invented in the early 1960s. However, laser development only recently progressed to the point that quantitative two-photon experiments can be performed with the confidence that the results can be reproduced in different laboratories. The development of high-power dye lasers pumped by YAG and excimer lasers has opened the door to new techniques for the detection of atoms and molecules. It has only been recognised in the last few years that two-photon processes could provide a sensitive detection technique, particularly for atomic species.

The need for a detection technique for determining absolute densities of atomic species such as H, C, N, O, S, and F under nonideal conditions (such as after the excitation of a laser gas mixture or in a combustion environment) has been well established for several years. It is difficult to detect these species using standard resonance fluorescence techniques under the most ideal conditions, and impossible under many of the hostile environments of interest today in laser, combustion, and plasma physics research.

The sensitive detection of atomic fluorine, coupled with good spatial and temporal resolution, would be particularly useful in a variety of research applications. Included among these are such diverse areas as plasma etching and vapor deposition processes for the semiconductor industry, excimer and chemical laser development, and research in fundamental chemical kinetics. In this report, we summarize the results of an AFOSR-sponsored research program to develop new detection techniques for atomic fluorine.

An ideal atomic fluorine detection technique would include the following characteristics: (1) good sensitivity ( $10^{12}$  to  $10^{13}$  cm $^{-3}$  desired), (2) good temporal resolution (10 to 100 ns) to resolve fast transient processes, (3) good spatial resolution (volumes of 0.1 mm $^3$  or less), (4) determination of species densities on an absolute scale, and (5) in situ detection that does not perturb the system under study. All these requirements can be met by a detection technique based on nonlinear optical processes.

This report is divided as follows: Section II summarizes of previous detection techniques for atomic F and outlines the general idea for the

application of two-photon excitation for F-atom detection, Section III summarizes the results of the research program (the reader is directed to the appendices for details) and Section IV presents recommendations for future research.

## BACKGROUND

### Non laser Detection Techniques

Reactions of atoms have long been investigated by absorption and resonance fluorescence using atomic resonance lamps as the photon source. Generally, these transitions are in the vuv portion of the spectrum and absorptions from molecular impurities are a major source of background interference. For atomic fluorine, the resonance transition occurs at 95 nm (which is beyond the LiF window cutoff), and hence the fluorescence cannot be readily detected. A complicated apparatus was developed by Clyne and Nip [CN77] for their F-atom resonance fluorescence experiments. The "window" they used in the experiment consisted of a collimated hole structure optimized for low gas conductance and high light transmission, and the experiment had to be differentially pumped. Because of these complications, we conclude that resonance fluorescence techniques are completely unsuitable as a general F-atom diagnostic.

### Single-Photon Laser Detection Techniques

Laser-based methods for F-atom detection were first proposed by Schlossberg [Sc76]. One of the techniques he proposed has recently been demonstrated at a level of sensitivity that makes it useful as an F-atom diagnostic. The technique consists of using IR diode lasers to probe the magnetic-dipole absorption transition at  $404\text{ cm}^{-1}$ . Details of this technique and estimated sensitivity limits are discussed in a report by Wormhoudt, Stanton and Silver [WSS83]. Although this development represents a major advance in F-atom detection, the sensitivity is relatively low ( $NL = 5 \times 10^{14}\text{ cm}^{-2}$ ), and the spatial resolution is limited to an average over the column density of F-atoms. We conclude that this technique does not have either the sensitivity or the spatial and temporal resolution needed for many of the potential applications.

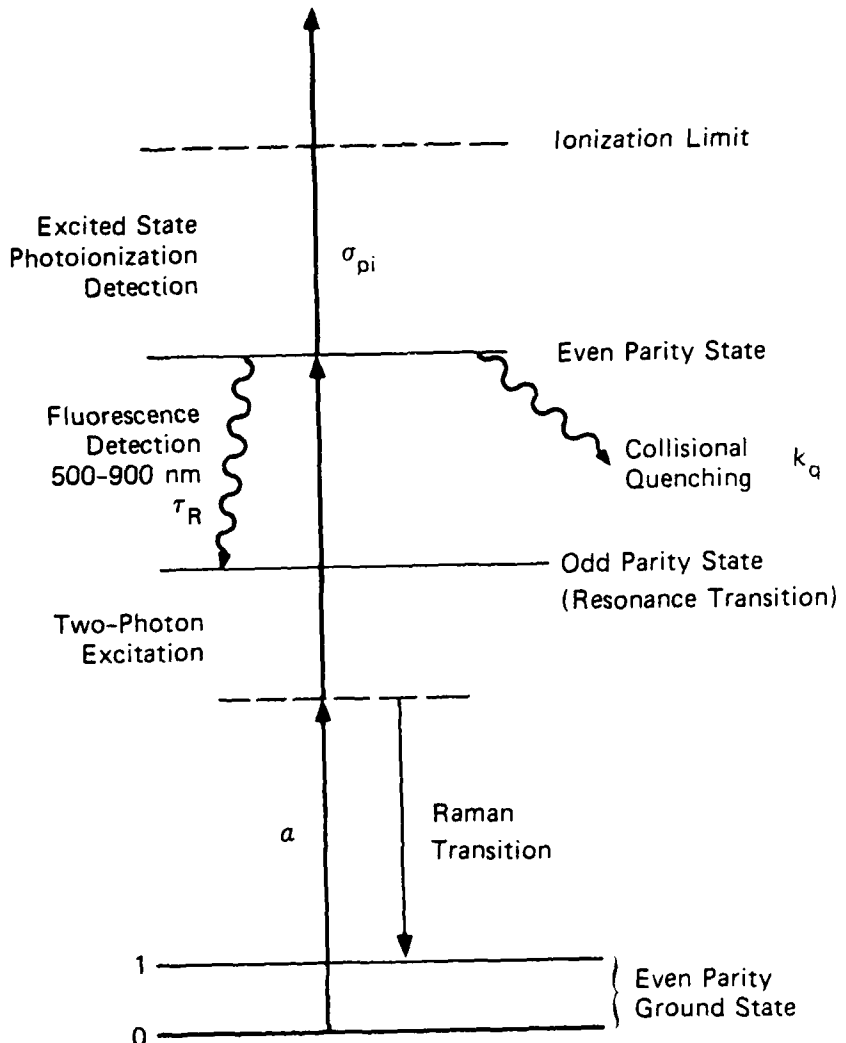
## Two-Photon Excitation Methods

Two types of two-photon transitions may be useful for detecting atoms. These are illustrated in Figure 1.

The first is a direct transition that accesses final states in the energy range of 65,000 to 120,000  $\text{cm}^{-1}$ . The occurrence of probe beam absorption or of fluorescence and ionization from the excited state forms the observed signal for these detection techniques. The fluorescence and ionization detection techniques are called two-photon excited fluorescence (TPEF) and two-photon resonant ionization spectroscopy (TPRIS) [see, for example, HPK 79]. The technique of TPEF is generally useful for applications where a remote detection capability is required because the fluorescence to be detected lies in the visible or near-IR region of the spectrum. The first experimental demonstration of TPEF was made at SRI International in 1981 for atomic oxygen and nitrogen [BCP81]. Demonstrations of TPEF and TPRIS for a number of atomic radicals quickly followed. All of the nonmetallic atomic radicals observed to date using this technique are listed in Table 1. Note that one of the most important radicals, atomic fluorine, has only been observed using the relatively insensitive techniques of infrared absorption spectroscopy (IRAS) and spontaneous Raman scattering (RS).

Several critical parameters need to be experimentally determined before this technique can be used to give absolute ground state number densities. These include the two-photon absorption cross section ( $\alpha$ ), the excited state radiative lifetimes ( $\tau_R$ ), collisional quenching rates ( $K_q$ ), and excited state photoionization cross sections ( $\sigma_{pi}$ ). These quantities are illustrated schematically in Figure 1.

The second type of two-photon transition illustrated in Figure 1 is a Raman transition where the final state energies range from 100 to 4000  $\text{cm}^{-1}$ . Only atoms that have their ground state split into their fine-structure components can be detected using this type of transition. Observation of the gain (or absorption) induced by the high-power pump laser on a CW probe laser forms the observed signal for this type of transition. This technique is called stimulated Raman gain spectroscopy (SRGS) and has been used to study several molecular systems [EO82]. Examples of atomic systems where this Raman-type transition may be useful for detection include F, C, O, and S.



JA-330583-25B

Figure 1. Generalized level diagram for the detection of atoms using two-photon excitation.

TABLE 1.

## LASER DETECTION OF ATOMIC RADICAL SPECIES

<u>Atom</u>	<u>Detection Method*</u>	<u>References</u>
H	TPRIS TPEF	ABF78; BAF78; Go82; ZRD81; HLW75; BFW81; LSK83
C( <sup>3</sup> P); C( <sup>1</sup> D)	TPEF	MEB81; DOV83
N	TPEF	BPC81; BPC82
O	TPEF BJB86; BDB87 TPRIS CARS RS	BPC81; BPC82; AEG82; Mi83; Go83 TB81 DB81
S( <sup>3</sup> P); S( <sup>1</sup> D)	TPEF and TPRIS	BVB82; VBD83
F	IRAS RS	SK80; LB82a CA79
Cl	TPEF CARS IRAS	HDJ88 HMF82 Mo82 DJM76; DR79
Br	IRAS CARS	KPC81 QM83
I( <sup>2</sup> P <sub>3/2</sub> ; <sup>2</sup> P <sub>1/2</sub> )	TPEF	BDO83

\*TPEF - two photon excited fluorescence, TPRIS - two photon resonant ionization spectroscopy, CARS - coherent anti-Stokes Raman spectroscopy, IRAS - infrared absorption spectroscopy, and RS - Raman Scattering. The last two are included for completeness.

Coherent anti-Stokes Raman spectroscopy (CARS) is related to SRGS and was originally proposed for F-atom detection by Schlossberg [Sc76]. This technique could have good sensitivity ( $10^{15} \text{ cm}^{-3}$ ) but suffers from the same problems as SRGS: the signal is proportional to the population difference ( $\Delta N$ ) (in CARS, the square of  $\Delta N$ ), not the absolute population (N). Both CARS and SRGS are most useful for systems in thermal equilibrium where the temperatures can be determined.

In the research reported here, we have only studied the direct two-photon excitation technique. Two-photon excitation (TPE) has several unique features that distinguish it from single-photon excitation processes. First, the fluorescence from the excited state will be in the visible or near-IR region of the spectrum where there are few interfering absorptions. Second, states can be excited at energies well above the limitation that window materials impose for single-photon excitation. This is particularly important for atomic fluorine. Third, because the two-photon Doppler width can be minimized or eliminated, thus enhancing the two-photon absorption coefficient can be enhanced. Fourth, the use of two lasers at different wavelengths and tight focal volumes allows extremely good spatial resolution to be obtained for cross-beam geometries. All these special features of TPE can be extremely useful.

## SUMMARY OF RESEARCH ACCOMPLISHMENTS

This section summarizes the results published in the papers included in the appendices.

### Two-Photon Detection of Atomic F

The basic concept for the TPEF technique is illustrated in Figure 2 for the fluorine atomic system. Electronic states in the region of  $118,000 \text{ cm}^{-1}$  are excited using a laser with a wavelength of 170 nm. The F atoms can then be detected by observing either visible fluorescence at 776 nm or ions produced by photoionization of the excited state. We have been particularly successful in developing the TPEF technique for O atom detection [HDJ88] and anticipate that the application of this technique to atomic F will yield similar detection sensitivities.

Figure 2 also illustrates that the detection technique could utilize lasers of two different wavelengths in the excitation process. The figure shows that one laser could be the fixed frequency  $F_2$  laser operating at 157 nm and the second laser could be a tunable laser operating at 185 nm (the wavelength necessary to meet the resonance condition). Because the detection sensitivity is proportional to the square of the laser intensity, the two-color experiment has the advantage that the high intensity  $F_2$  laser could be used to increase the detection sensitivity although the experiment would be somewhat more complicated.

The experimental apparatus developed for these experiments is illustrated in Figure 3. The most difficult aspect of the experiment is the generation of the 170-nm radiation at sufficient intensity to produce an observable fluorescence signal. A series of experiments were performed to determine whether we could generate this vuv wavelength using multiwave Raman mixing in  $H_2$ . We were able to demonstrate that more than  $10 \mu\text{J}$  of energy can be obtained at 170 nm when a standard YAG pumped dye laser doubled to the UV giving an energy of 30 mJ at 280 nm is used as the pump laser. The output from the Raman cell in Figure 3 is collimated using a  $\text{CaF}_2$  lens, and the anti-

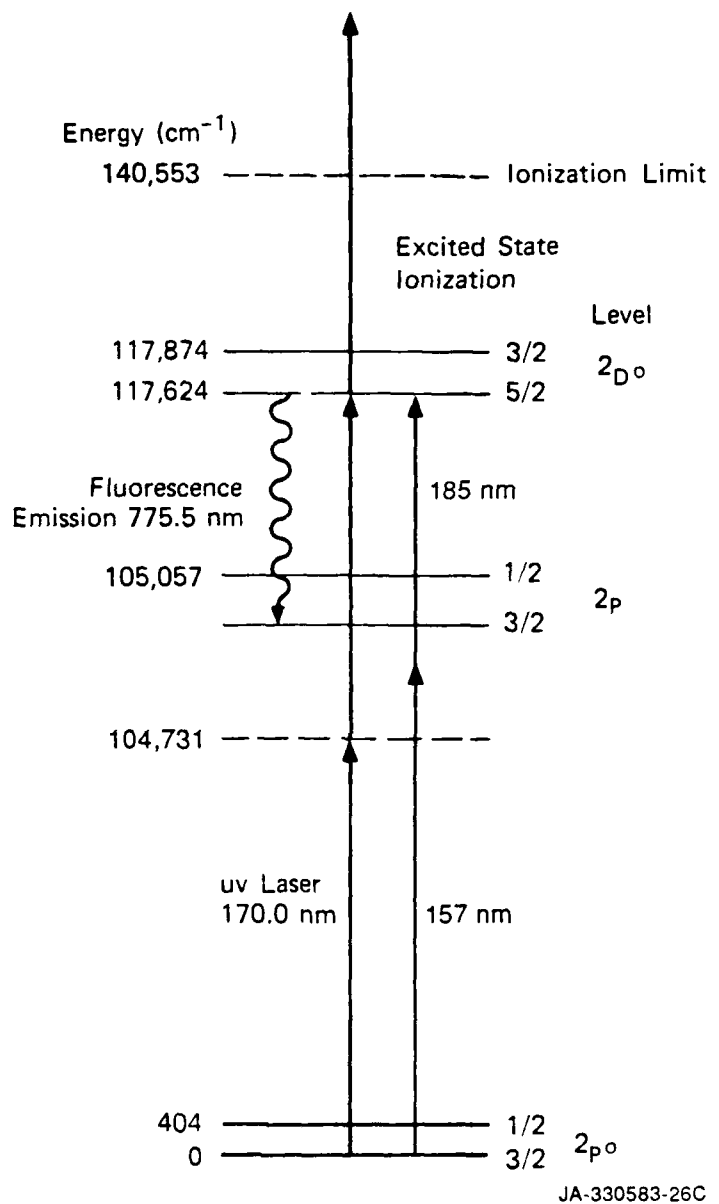
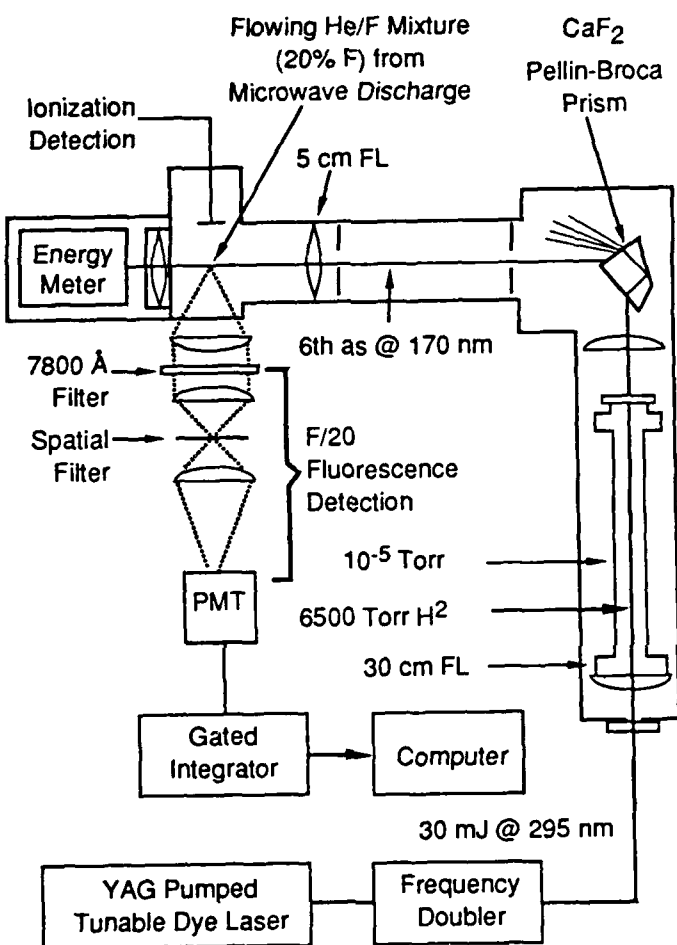


Figure 2. Fluorine excited states relevant to the two-photon detection technique.



JA-8320-18C

Figure 3. Experimental apparatus for the detection of atomic fluoresce using the TPEF technique.

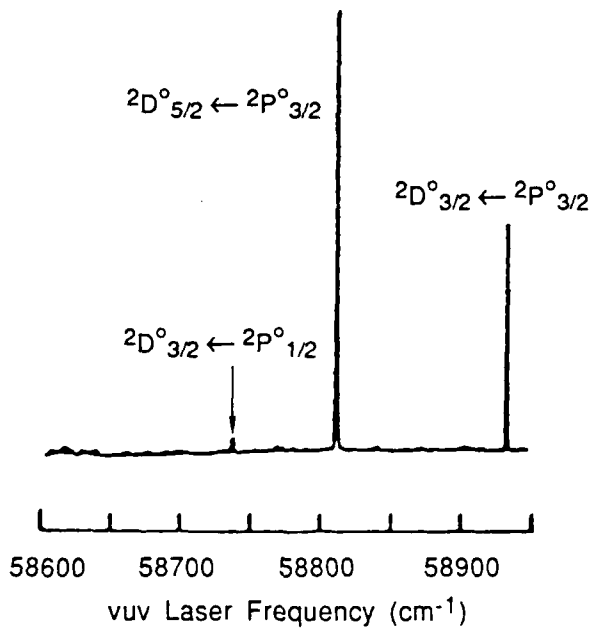
Stokes (AS) orders are separated using a  $\text{CaF}_2$  Pellin-Broca prism. The sixth AS at 170 nm is propagated through an evacuated beam path ( $10^{-5}$  torr) and focused into the experimental cell using a 5-cm focal length  $\text{CaF}_2$  lens. The light is then recollimated and detected by a pyroelectric energy meter to monitor the absolute energy in the cell.

The F atoms are produced by flowing a mixture of 10%  $\text{F}_2$  in He through a microwave discharge. By observing the decrease in the resonantly-enhanced multiphoton ionization (REMPI) signal from  $\text{F}_2$  (see Appendix B) we have verified that more than 90% of the  $\text{F}_2$  is dissociated in the discharge.

Ions are collected using a set of two electrodes in the cell biased at 90 V, and the charge is amplified using a charge preamplifier. We also observed fluorescence at 776 nm from the excitation volume using an F/2 collection lens, a spatial filter to reject scattered light, a 50% transmitting filter at 776 nm, and an RCA C31034A photomultiplier tube.

An example of the experimental data is given in Figure 4 where we have plotted relative fluorescence intensity at 776 nm as a function of laser frequency. The excited state is the  $^2\text{D}_{5/2,3/2}$  illustrated in Figure 2 at  $118,000 \text{ cm}^{-1}$ . We expected and observed four transitions (see Figure 2): two from the  $^2\text{P}_{3/2}$  ground state, one to (1) the  $^2\text{D}_{3/2}$  with  $\nu_1 = 58,936.5 \text{ cm}^{-1}$ , and one to (2) the  $^2\text{D}_{5/2}$  with  $\nu_1 = 58,811.5 \text{ cm}^{-1}$ ; and two from the  $^2\text{P}_{1/2}$  (the upper fine-structure level of the ground state) one to (3) the  $^2\text{D}_{3/2}$  with  $\nu_1 = 58,734.4 \text{ cm}^{-1}$  and one to (4) the  $^2\text{D}_{5/2}$  with  $\nu_1 = 58,609.4 \text{ cm}^{-1}$ . These data are unambiguous evidence that we are indeed observing atomic fluorine. The relative intensities of the four transitions are proportional to the population on each of the two fine-structure ground states (determined by the temperature of the gas at the observation volume) as well as the relative two-photon absorption cross sections and the laser intensity. The relative two-photon cross section determined from these data are given in Appendix A.

Radiative lifetimes and quenching rates for the excited states can now be measured by observing the time dependence of the fluorescence at 776 nm. These data are important for determining the fluorescence quantum efficiency and hence relative ground state populations. These data are also given in Appendix A.



JA-8320-16

Figure 4. Two-photon excited fluorescence intensity at 776 nm.

We believe that the development of two-photon detection techniques for atomic fluorine will have important applications in the diagnostics of the reacting flows. The work presented here and in Appendix A is first demonstration that the technique of TPEF can be used to study atomic fluorine using a relatively simple experimental apparatus.

#### Three-Photon Resonantly Enhanced Multiphoton Ionization of F

Three-photon excitation with the subsequent observation of fluorescence has been used successfully to detect H atoms and may prove to be useful in the detection of F as well. The main advantage of the three-photon excitation scheme is that it requires a laser wavelength in the region of 220 to 286 nm, depending on what level is excited. Since these wavelengths can be generated using standard nonlinear techniques with millijoules of energy, there is a big advantage to be gained in the simplicity of the experiment. We therefore set up an experiment to observe the first multiphoton excitation spectra of F.

The results of this experiment are given in Appendix B, and the most important points are summarized here. Since we wanted to obtain the largest signal-to-noise ratio for this first experiment, we decided to use the ionization signal rather than a fluorescence signal to monitor the multiphoton excitation process. From these experiments, we reported the first observation of resonantly-enhanced multiphoton ionization (REMPI) of atomic fluorine. Four excited states were observed in the region of  $105,000 \text{ cm}^{-1}$  corresponding to the  $^2\text{P}_{1/2,3/2}^0 \rightarrow ^2\text{P}_{1/2,3/2}$  three-photon transition in a 3+2 photon ionization process. The dye laser wavelength used in these experiments was 286 nm. We also observed REMPI spectra of  $\text{F}_2$  in a 3+1 photon process. Using absorption spectra from the literature, we have identified the resonant excited states as  $\text{H}^1\Sigma_u$  and  $\text{h}^3\Sigma_{1,u}$ . We estimated that the F-atom detection sensitivity of this experiment was  $\sim 10^{12} \text{ cm}^3$ .

The stronger than anticipated signals in the experiment indicate that three-photon excitation may be a viable alternative to two-photon excitation for remote detection applications of F.

Three-photon excitation may also be a viable technique for populating high-lying states in atomic F that fluoresce. Whether these states are populated can be determined by observing the 3+1 REMPI spectrum. For the 3+1 REMPI experiments, we chose to excite  $3d^2\text{P}_j$  state at  $128,000 \text{ cm}^{-1}$ . The

experiment consisted of tuning a laser to 233 nm and observing the ionization signal while searching for fluorescence in the region of 700 to 800 nm. A gas mixture (5% F<sub>2</sub> in He) was flowed through a cell equipped with an electrode for monitoring the total ion current and with collection optics for monitoring the fluorescence in the region of 700 to 800 nm. We mixed the frequency-doubled output of a tunable dye laser with a 1.06-μm YAG output to produce the tunable 233-nm light. This light is used for both the photodissociation of the F<sub>2</sub> and REMPI of the F.

With this apparatus, we obtained the first 3+1 REMPI ionization spectra in the 233-nm region. The spectra show lines where most of the atomic fluorine lines are expected to be and also contain extra lines that may be due to impurities in the compound. All these lines lie on top of a background signal that is wavelength independent and produced the dominant noise. The fluorine lines show a roughly linear relationship to with gas density, whereas the impurity lines are somewhat independent of gas pressure.

We were unable to detect any clear sign of fluorescence from any of the intermediate fluorine states. We detected very weak fluorescence signals for the laser wavelength regions where the strongest ionization lines appear, but this fluorescence signal may be due to one of the impurity lines. Since we were able to observe only two fluorescence lines, we cannot unambiguously assign them to the expected atomic F spectrum. Although the ionization signals are relatively large, it appears that three-photon excitation followed by the detection of fluorescence will not be a sensitive detection technique for atomic F. Further research with larger F-atom densities is necessary to determine if the fluorescence that was observed can be assigned to F- transitions.

#### Experiments Using Time-of-Flight Mass Spectrometer

Because impurity signals precluded a clear analysis of the fluorine ion spectrum in all our REMPI experiments, we decided to build a time-of-flight (TOF) mass spectrometer to aid in the analysis of the fluorine REMPI data. The atomic fluorine beam developed for the TOF spectrometer might also be usable as the high-density atomic F source in our fluorescence detection experiments.

The TOF spectrometer is used in conjunction with a pulsed gas jet that allows the highest possible gas densities in the probing volume and the lowest possible densities at the detector. The 20-cm free-flight region gives a mass resolution of approximately 50 for our simple TOF mass spectrometer design.

With the TOF apparatus, we again obtained the  $3s^2 P_J$  spectrum at 285 nm. We found that the 3+1 REMPI of  $F_2$  at 284 nm produces only  $F^+$  and no  $F_2^+$  within the sensitivity limits of our detector. This result implies that the ionization of  $F_2$  is immediately followed by the photodissociation of  $F_2^+$  and thus the TOF mass spectrometer is unable to separate the  $F^+$  and the  $F_2^+$  spectra. Additional details of this work are described in Appendix C.

## CONCLUSIONS AND RECOMMENDATIONS

We have demonstrated that atomic fluorine can be remotely detected with good sensitivity using two-photon excited laser-induced fluorescence (TPEF) at 170 nm. Future work in this area should include experimental and theoretical work to calibrate the fluorescence signals to determine absolute ground state densities. This would require the following:

- (1) Measurement of the two-photon cross section.
- (2) Measurement of quenching rates of the  $^2D_J$  states by various collision particles.
- (3) Development of a high-power laser source at 170 nm to improve sensitivity as well as to provide the energy necessary for 2-dimensional imaging of F-atom distributions.

## PUBLICATIONS AND CONFERENCE PRESENTATIONS

The following publications have resulted from this work:

1. "Two-photon-excited fluorescence spectroscopy of atomic fluorine at 170 nm," Gregory C. Herring, Mark J. Dyer, Leonard E. Jusinski, and William K. Bischel, Opt. Lett. 13, 360 (1988).
2. "Multiphoton ionization spectroscopy of atomic fluorine," William K. Bischel and Leonard E. Jusinski, Chem. Phys. Lett. 120, 337 (1985).
3. "Two-Photon spectroscopy of atomic fluorine and oxygen," W. K. Bischel, D. J. Bamford, M. J. Dyer, G. C. Herring, and L. E. Jusinski, Laser Spectroscopy III, eds. W. Persson and S. Svanberg, pg. 178 (Springer-Verlag, Berlin, 1987).
4. "Mechanisms for F<sup>+</sup> production in the multiphoton ionization of F<sub>2</sub>," Gregory C. Herring, Leonard E. Jusinski, Mark J. Dyer, and William K. Bischel, prepared for submission to Phys. Rev. A (1988).

The research has been reported at the following conferences:

1. "Multiphoton ionization spectroscopy of atomic fluorine," William K. Bischel and Leonard E. Jusinski, presented at the Annual Meeting of the Optical Society of America, October 14-18, 1985, Washington DC.
2. "Multiphoton detection techniques for atomic fluorine," William K. Bischel, presented at the 1986 AFOSR Contractors' Meeting, June 16-17, 1986, Stanford University, Stanford, CA.
3. "Multiphoton ionization spectroscopy of F and F<sub>2</sub> using a time-of-flight mass spectrometer," Gregory C. Herring, Leonard E. Jusinski, Mark J. Dyer, and William K. Bischel, presented at CLEO/IQEC '87 April 27 - May 1, 1987, Baltimore, MD.

4. "Mechanisms for F<sup>+</sup> production in the multiphoton ionizaton of F<sub>2</sub>," Gregory C. Herring, Leonard E. Jusinski, Mark J. Dyer, and William K. Bischel, presented at the 18th Annual Meeting of the Division of Atomic, Molecular, and Optical Physics, May 18-20, 1987, Cambridge, MA.
5. "Two-photon spectroscopy of atomic fluorine and oxygen," William K. Bischel, Douglas J. Bamford, Mark J. Dyer, Gregory C. Herring, and Leonard E. Jusinski, presented at the 8th International Conference on Laser Spectroscopy, June 22-26, 1987, Are, Sweden.
6. "Two-photon excited fluorescence and three-photon ionization of atomic fluorine at 170 nm," Gregory C. Herring, Mark J. Dyer, Leonard E. Jusinski, and William K. Bischel, presented at the 3rd International Laser Science Conference, November 1-5, 1987, Atlantic City, NJ.

## REFERENCES

ABF78 C. P. Ausschnit, G. C. Bjorklund, and R. R. Freeman, Appl. Phys. Lett. 33, 54 (1978).

AEG82 M. Alden, H. Edner, P. Grafstrom, and S. Svanberg, Opt. Comm. 42, 244 (1982).

BAF78 G. C. Bjorklund, C. P. Ausschnit, R. R. Freeman, and R. U. Storz, Appl. Phys. Lett. 33, 54 (1978).

BDB87 D. J. Bamford, M. J. Dyer, and W. K. Bischel, Phys. Rev. A 36, 3497 (1987).

BDO83 P. Brewer, P. Das, G. Ondrey, and R. Bersohn, J. Chem. Phys. 79, 720 (1983).

BFW81 J. Bokor, R. R. Freeman, R. L. Panock, and J. C. White, Opt. Lett. 6, 182 (1981).

BJB86 D. J. Bamford, L. E. Jusinski, and W. K. Bischel, Phys. Rev. A 34, 185 (1986).

BPC81 W. K. Bischel, B. E. Perry, and D. R. Crosley, Appl. Opt. 21, 1419 (1982); Chem. Phys. Lett. 82, 85 (1981).

BVB82 P. Brewer, N. Van Veen, and R. Bersohn, Chem. Phys. Lett. 91, 126 (1982).

CA79 J. C. Cummings and D. P. Aeschliman, Opt. Comm. 3, 165 (1979).

CN77 M.A.A. Clyne and W. S. Nip, JCS Faraday Trans. II, 73, 1308 (1977).

DB81 C. J. Dasch asnd J. J. Bechtel, Opt. Lett. 6, 36 (1981).

DJM76 M. Dagenais, J.W.C. Johns, and A.R.W. McKellar, Can. J. Phys. 54, 1438 (1976).

DOV83 P. Das, G. Ondrey, N. Van Veen, and R. Bersohn, J. Chem. Phys. 79, 724 (1983).

DR793 P. B. Davies and D. K. Russell, Chem. Phys. Lett. 67, 40 (1979).

E082 P. Eggerick and A. Owyoungm, "High Resolution Stimulated Raman Spectroscopy," in Advances in Infrared and Raman Spectroscopy Vol 9, R. J. H. CLark and R. E. Hestor, Eds. (Heydon and Son Ltd., Londond, 1982).

Go82 J.E.M. Goldsmith, Opt. Lett. 7, 437 (1982).

Go83 J.E.M. Goldsmith, J. Chem. Phys. 78, 1610 (1983).

HDJ88 G. C. Herring, M. J. Dyer, L. E. Jusinski, and W. K. Bischel, Opt. Lett. 13, 360 (1988).

HLW75 T. W. Hansch, S. A. Lee, R. Wallenstein, and C. Wieman, Phys. Rev. Lett. 34, 307 (1975).

HMF82 M. Heaven, T. A. Miller, R. R. Freeman, J. C. White, and J. Bokor, Chem. Phys. Lett. 786, 458 (1982).

HPK79 G. S. Hurst, M. G. Payne, S. D. Kramer, and J. P. Young, Rev. Mod. Phys. 61, 767 (1979).

KPC81 J.V.V. Kasper, C. R. Pollack, R. F. Curl, Jr., and F. K. Tittel, Chem. Phys. Lett. 77, 211 (1981).

LB82a G. A. Laguna and W. H. Beattie, Chem. Phys. Lett. 88, 439 (1982).

LSK83 R. P. Lucht, J. T. Salmon, G. B. King, D. W. Sweeney, and N. M. Laurendeau, Opt. Lett. 7, 365 (1983).

MEB81 C. H. Muller III, D. R. Eames, and K. H. Burrell, Bull. Am. Phys. Soc. 26, 1031 (1981).

Mi83 A. Mizolek, Annual Meeting Opt. Soc. Am. New Orleans, October 17-20 (1983)

Mo82 D. S. Moore, Chem. Phys. Lett. 89, 131 (1983).

QM83 C. R. Quick and D. S. Moore, J. Chem. Phys. 79, 759 (1983).

Sc76 H. Schlossberg, J.A.P. 47, 2044 (1976).

SK80 A. C. Stanton and C. E. Kolb, J. Chem. Phys. 72, 6637 (1980) and Laser Focus March 1983, p. 44.

TB81 R. E. Teets and J. H. Bechtel, Opt. Lett. 6, 458 (1981).

VBD83 W. Van Veen, P. Brewer, P. Das, and K. Bersohn, J. Chem. Phys. 79, 4295 (1983).

WSS83 J. Wormhoudt, A. C. Stanton, and J. Silver, Spectroscopy Characterization Techniques for Semiconductive Technology Vol. 452, proceedings SPIE (1983).

ZRD81 H. Zacharias, H. Rottke, J. Danon, and K. H. Welge, Opt. Com. 37, 15 (1981).

APPENDIX A

TWO-PHOTON-EXCITED FLUORESCENCE SPECTROSCOPY OF ATOMIC FLUORINE AT 170 nm

## APPENDIX A

## Two-photon-excited fluorescence spectroscopy of atomic fluorine at 170 nm

G. C. Herring,\* Mark J. Dyer, Leonard E. Jusinski, and William K. Bischel

*Chemical Physics Laboratory, SRI International, Menlo Park, California 94025*

Received October 20, 1987; accepted January 26, 1988

We report what is to our knowledge the first two-photon-excited fluorescence spectroscopy of atomic fluorine. A doubled dye laser at 286 nm is Raman shifted in H<sub>2</sub> to 170 nm (sixth anti-Stokes order) to excite ground-state '<sup>3</sup>P<sub>j</sub>' fluorine atoms to the '<sup>2</sup>D<sub>j</sub>' level. The fluorine atoms are detected by one of two methods: observing the fluorescence decay to the '<sup>2</sup>P<sub>j</sub>' level or observing F\* production through the absorption of an additional photon by the excited atoms. We have measured relative two-photon absorption cross sections to and the radiative lifetimes of the '<sup>2</sup>D<sub>j</sub>' states.

The remote detection of atomic fluorine with high sensitivity, coupled with good temporal and spatial resolution, is an important unsolved problem. Three optical detection techniques have been reported in the literature: infrared absorption on the forbidden  $^2P_{1/2} \leftarrow ^2P'_{3/2}$  ground-state fine-structure transition<sup>1,2</sup> at 404 cm<sup>-1</sup>, VUV absorption<sup>3</sup> on the resonance transition at 95 nm, and spontaneous Raman scattering<sup>4</sup> at 404 cm<sup>-1</sup>. Since the sensitivity and the temporal and spatial resolution cannot be simultaneously optimized for these techniques, they have only a limited range of application. Although coherent anti-Stokes Raman spectroscopy has been proposed<sup>2</sup> as a detection technique, it has been demonstrated only for the halogen atoms Br (Ref. 5) and Cl (Ref. 6) with limited sensitivity<sup>6</sup> (densities  $\geq 10^{15}$  atoms/cm<sup>3</sup>). Therefore a new F atom detection technique needed to be developed that would be suitable for the many demanding applications in laser development and semiconductor processing.<sup>7</sup>

The technique of two-photon excited fluorescence<sup>8</sup> (TPEF) can, in principle, have high sensitivity coupled with excellent temporal and spatial resolution. TPEF was first demonstrated in 1981 for the light atomic radicals of O,<sup>8</sup> N,<sup>8</sup> and H.<sup>9</sup> The technique has since been applied to the detection of C,<sup>10</sup> S,<sup>11</sup> Cl,<sup>12</sup> and I.<sup>13</sup> Of the light radical atoms, only fluorine has yet to be detected using this technique.

In this Letter we report the first observation to our knowledge of two-photon excited fluorescence (at 776 or 780 nm) from F atoms using an excitation laser wavelength of 170 nm. The basic concept for the TPEF technique is illustrated in Fig. 1 for the F atomic system. Electronic states in the region of 118 000  $\text{cm}^{-1}$  are excited by using a laser with a wavelength of 170 nm. The F atoms can then be detected by observing visible fluorescence at 776 nm or by observing ions produced by photoionization of the excited state. We have been particularly successful in developing the TPEF technique for O atom detection<sup>8,14,15</sup> and anticipate that the application of this technique to atomic F should yield similar detection sensitivities.

The experimental apparatus is illustrated in Fig. 2. We generate radiation at 170 nm by using multiwave

Raman mixing in H<sub>2</sub>. A standard YAG-pumped dye laser (Quanta-Ray DCR-2A and PDL-2) is doubled (Inrad AT II) to the UV, giving an energy of 30 mJ at 295 nm. Both the visible and the UV laser beams are focused into the Raman cell with a 30-cm focal-length lens. The resulting energy in the sixth anti-Stokes wave at 170 nm is usually between 5 and 10  $\mu$ J (2.5 nsec FWHM). With the Raman cell at room temperature and 6500 Torr, we exchange the H<sub>2</sub> in the Raman cell once every 30 min to prevent laser-induced breakdown of impurities at the focal point. The output from the Raman cell in Fig. 2 is collimated using a CaF<sub>2</sub> 25-cm focal-length lens, and the anti-Stokes (AS) orders are separated using a CaF<sub>2</sub> Pellin-Broca prism. The sixth AS wave at 170 nm is propagated through a series of baffles in an evacuated beam path (10<sup>-5</sup> Torr) and focused into the experimental cell by using a 5-cm focal-length CaF<sub>2</sub> lens. Another CaF<sub>2</sub> lens is used as the exit window of the cell and to recollimate the 170-nm beam before it is detected by a pyroelectric energy meter.

The F atoms are produced by flowing  $F_2/He$  (10%  $F_2$ ) through a microwave (2450-MHz) discharge that takes place inside a 9-mm i.d. alumina tube.<sup>1</sup> The alumina tube is oriented perpendicular to the 170-nm

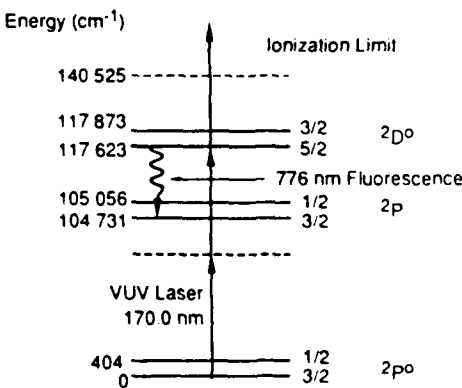


Fig. 1. F-atom excited states relevant to the two-photon detection technique.

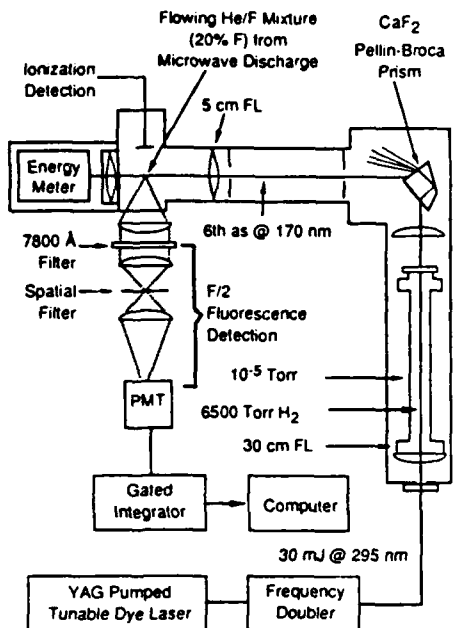


Fig. 2. Experimental apparatus for the two-photon excitation of atomic F followed by the detection of ionization and fluorescence.

laser beam, and the focus of the laser is 5–10 mm away from the exit of the tube. The flow speed through the tube is approximately  $2 \times 10^3$  cm/sec, and the distance between the end of the Eversole-type discharge cavity and the laser focus is approximately 15 cm. We estimate that more than 80% of the  $F_2$  is dissociated in the discharge by observing the disappearance of the resonantly enhanced multiphoton ionization (REMPI) signal<sup>16</sup> from  $F_2$  when the discharge is started. A Chromel-Alumel thermocouple, inserted into the flow, is used to determine that the temperature of the F/He flow (typically 7-Torr total pressure) at the laser focus is 303 K.

Both the ion and the fluorescence spectra were obtained by averaging (1-sec time constant) with boxcar integrators, while the fluorescence time decays were obtained by sending the photomultiplier tube (plus preamplifier) signal directly to a Tektronix 2430 digital oscilloscope (150-MHz bandwidth). Ions are collected by using a set of two electrodes (9-mm separation) biased at 90 V, and the collected charge is amplified using an Ortec Model 142 PC charge-integrating preamplifier. After the ion electrodes are removed, fluorescence at 776 and 780 nm can also be observed (perpendicular to both the exciting 170-nm beam and the alumina discharge tube) from the excitation volume by using  $f/2$  collection optics, a spatial filter (1 mm  $\times$  1 mm aperture) to reject scattered light, a 50% transmitting filter at 776 nm, and an RCA C31034A photomultiplier tube. The collection solid angle for the fluorescence was about 0.15 sr, and the net magnification from the focal region to the aperture is unity.

An example of the experimental data is given in Fig.

3, where the fluorescence intensity at 776 nm is plotted as a function of VUV laser frequency. The excited states are the  $^2D_{5/2,3/2}$  illustrated in Fig. 1 at 118 000  $\text{cm}^{-1}$ . We expect and observe four transitions (see Fig. 1): (1)  $^2D_{3/2} \leftarrow ^2P_{3/2}$  (58 936.5  $\text{cm}^{-1}$ ), (2)  $^2D_{5/2} \leftarrow ^2P_{3/2}$  (58 811.5  $\text{cm}^{-1}$ ), (3)  $^2D_{3/2} \leftarrow ^2P_{1/2}$  (58 734.4  $\text{cm}^{-1}$ ), and (4)  $^2D_{5/2} \leftarrow ^2P_{1/2}$  (58 609.4  $\text{cm}^{-1}$ ). Transitions (1)–(3) are clearly above the noise in Fig. 3, and we have observed transition (4) with optimized scans. The signal-to-noise ratios of our 2 + 1 REMPI signals are comparable with the fluorescence spectra of Fig. 3.

The two-photon transition is expected to be Doppler broadened with a FWHM linewidth of 0.34  $\text{cm}^{-1}$  at 300 K. The measured FWHM linewidth is  $\sim 3 \text{ cm}^{-1}$  (in two-photon frequency units). This implies a linewidth for the sixth AS radiation of  $\sim 2 \text{ cm}^{-1}$ , a linewidth that is substantially larger than the doubled-dye-laser linewidth estimated to be  $\sim 0.6 \text{ cm}^{-1}$ . The broadening of the AS linewidth is primarily due to the ac Stark effect in  $H_2$  during the stimulated Raman process.<sup>17</sup>

We have measured the intensity dependence of the fluorescence and ion signals in our experiment for transitions (1) and (2). The fluorescence signals exhibit the expected quadratic dependence on the laser energy, while the ion signals have nearly cubic dependences ( $n = 2.7$ ). This result implies that the ionization step in the 2 + 1 REMPI process may be slightly saturated under our experimental conditions.

We have also measured the relative two-photon absorption cross sections for the four transitions to the  $^2D_{5/2,3/2}$  states. The measured relative peak heights (see Fig. 3) are corrected for lower-state population differences (assuming a Boltzmann population distribution at our measured gas temperature of 303 K), laser energies, and fluorescence branching ratios to determine relative two-photon absorption cross sections. The results are given in Table 1.

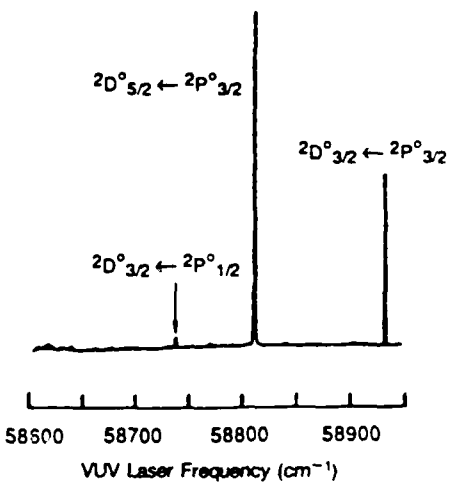


Fig. 3. Relative fluorescence intensity at 776 and 780 nm as a function of laser frequency following the two-photon excitation of the  $^2D_j$  excited state. Three peaks are observed at this sensitivity level corresponding to transitions among the four states illustrated in Fig. 1.

**Table 1. Summary for Measurements of Atomic Fluorine Two-Photon Absorption Cross Sections for the Transitions  $^2D_{5/2,3/2} \leftarrow ^2P_{3/2,1/2}$**

Two-Photon Transition ( $J_f \leftarrow J_i$ )	Initial State Population ( $T = 303$ K)	Relative Two-Photon Cross Sections	
		Theory	Experiment
$5/2 \leftarrow 3/2$	0.932	1.0	$1.0 \pm 0.2$
$3/2 \leftarrow 3/2$	0.932	0.43	$0.6 \pm 0.2$
$5/2 \leftarrow 1/2$	0.068	0.57	$0.9 \pm 0.3$
$3/2 \leftarrow 1/2$	0.068	0.86	$0.9 \pm 0.3$

The two photon absorption cross section  $\sigma_0^{(2)}$  ( $J' \leftarrow J$ ), in units of  $\text{cm}^4$ , can be calculated from<sup>18</sup>

$$\sigma_0^{(2)}(J' \leftarrow J) = \frac{F}{2J+1} \sum_M \left| \sum_{M_L} \langle LM_L | S(M - M_L) | JM \rangle \langle L'M_L | S(M - M_L) | J'M \rangle A_{LL}(M_L) \right|^2, \quad (1)$$

where  $F = (2\pi)^3 (e^2/\hbar c)^2 (\hbar\omega)^2$ ,  $\omega$  is the laser frequency, the  $\langle \cdot \rangle$  denote standard Clebsch-Gordan coefficients, and  $A_{LL}(M_L)$  is defined as

$$A_{LL}(M_L) = \sum_k \frac{\langle L'M_L | z | k \rangle \langle k | z | LM_L \rangle}{E_{LM_L} - E_k + \hbar\omega}, \quad (2)$$

where  $|k\rangle$  is any complete set of states and  $E_k$  is the energy of the  $|k\rangle$  state. In Eqs. (1) and (2) we have expanded the  $|JM\rangle$  states in terms of  $|LM_L S M_S\rangle$  states and assumed linear polarization ( $M' = M$ ). For the  $\Delta L = 1$   $^2D^o \leftarrow ^2P^o$  multiplet transition, the  $A_{2,1}(0)$  term is identically zero, and hence the relative two-photon cross sections for the four transitions illustrated in Fig. 1 can be calculated from Eq. (1) without calculating  $A_{2,1}(1)$ . The results of these calculations are compared with our measurements in Table 1. We see that the theoretical and experimental values for the relative two-photon cross sections agree to within the estimated experimental error limits of 20–30%.

The absolute two-photon cross section can also be estimated<sup>18</sup> by using Eqs. (1) and (2) if it is assumed that only the  $3s$   $^2P$  state at  $105\,000\text{ cm}^{-1}$  contributes to the two-photon matrix element. Using the oscillator strengths for the  $3s$   $^2P \leftarrow p^5$   $^2P^o$  resonance transition<sup>3</sup> at 95 nm and our measurement of the  $3p$   $^2D^o \leftarrow 3s$   $^2P$  radiative lifetime (see below), we calculate<sup>18</sup> that  $\sigma_0^{(2)} = 2.7 \times 10^{-36}\text{ cm}^4$  for the  $J' = 5/2 \leftarrow J'' = 3/2$  transition. It is interesting to note that this cross section is 3.1 times smaller than the largest two-photon cross section in atomic oxygen.<sup>15,18</sup>

Finally, we have measured the radiative lifetime and quenching rate for both fine-structure levels of the  $^2D_J$  state by observing the time dependence of the fluorescence at 776 and 780 nm. The slope of the linear least-squares fit to the measured decay rates as a function of pressure gives the combined He/F quenching rate, and the zero pressure intercept gives the lifetime of the excited  $^2D_{5/2,3/2}$  states. Our measured quenching rates

are  $1.3 \pm 0.1$  and  $2.3 \pm 0.1 \times 10^{-10}\text{ cm}^3\text{ sec}^{-1}$  for the  $J = 3/2$  and  $J = 5/2$  states, respectively. The average lifetime for the excited  $^2D_J$  states is  $27 \pm 1$  nsec (one standard deviation) and is approximately 15% smaller than previous measurements.<sup>19–22</sup>

We believe that the development of two-photon detection techniques for atomic F will have important applications in the diagnostics of reacting flows<sup>2</sup> as well as in basic excited state spectroscopy. The results presented here are the first known demonstration that the relatively simple technique of TPEF is viable for quantitative detection of atomic F.

This research was supported by the U.S. Air Force Office of Scientific Research under contract no. F49520-85K-0005. We thank Douglas J. Bamford for help in the development of the laboratory apparatus. W. K. Bischel thanks R. P. Saxon for stimulating conversations concerning the calculation of relative two-photon cross sections.

\*Current address, NASA Langley Research Center, Hampton, Virginia 23665-5225.

## References

1. A. C. Stanton, and C. E. Kolb, *J. Chem. Phys.* **72**, 6637 (1980).
2. H. Schlossberg, *J. Appl. Phys.* **47**, 2044 (1976).
3. M. A. A. Clyne and W. S. Nip, *J. Chem. Soc. Faraday Trans. 2* **73**, 1308 (1977).
4. J. C. Cummings and D. P. Aeschliman, *Opt. Commun.* **31**, 165 (1979).
5. C. R. Quick, Jr., and D. S. Moore, *J. Chem. Phys.* **79**, 759 (1983).
6. D. S. Moore, *Chem. Phys. Lett.* **89**, 131 (1982).
7. G. L. Loper and M. D. Tabat, *Appl. Phys. Lett.* **46**, 654 (1985).
8. W. K. Bischel, B. E. Perry, and D. R. Crosley, *Chem. Phys. Lett.* **82**, 85 (1981).
9. J. Bokor, R. R. Freeman, J. C. White, and R. H. Storz, *Phys. Rev. A* **24**, 612 (1981).
10. C. H. Muller III, D. R. Eames, and K. H. Burrell, *Bull. Am. Phys. Soc.* **26**, 1031 (1981); P. Das, G. Ondrey, N. van Veen, and R. Bersohn, *J. Chem. Phys.* **79**, 724 (1983).
11. P. Brewer, N. Van Veen, and R. Bersohn, *Chem. Phys. Lett.* **91**, 126 (1982).
12. M. Heaven, T. A. Miller, R. R. Freeman, J. C. White, and J. Bokor, *Chem. Phys. Lett.* **86**, 458 (1982).
13. P. Brewer, P. Das, G. Ondrey, and R. Bersohn, *J. Chem. Phys.* **79**, 720 (1983); J. J. Tice, M. J. Ferris, G. W. Loge, and F. B. Wompler, *Chem. Phys. Lett.* **96**, 422 (1983).
14. D. J. Bamford, L. E. Jusinski, and W. K. Bischel, *Phys. Rev. A* **34**, 185 (1986).
15. D. J. Bamford, M. J. Dyer, and W. K. Bischel, *Phys. Rev. A* **36**, 3497 (1987).
16. W. K. Bischel and L. E. Jusinski, *Chem. Phys. Lett.* **120**, 337 (1985).
17. W. K. Bischel, D. J. Bamford, and M. J. Dyer, *Proc. Soc. Photo-Opt. Instrum. Eng.* **912** (to be published).
18. R. P. Saxon and J. Eichler, *Phys. Rev. A* **34**, 199 (1986).
19. M. I. Burshtein, *Opt. Spectrosc. (USSR)* **55**, 464 (1983).
20. V. Lokner, C. Vadla, and V. Vujićević, *J. Quant. Spectrosc. Radiat. Transfer* **30**, 187 (1983).
21. G. Baruscha and E. Schulz-Gulde, *Astron. Astrophys.* **44**, 335 (1980).
22. R. D. Bengtson, M. H. Miller, D. W. Koopman, and T. D. Wilkerson, *Phys. Rev. A* **3**, 16 (1971).

APPENDIX B

MULTIPHOTON IONIZATION SPECTROSCOPY OF ATOMIC FLUORINE

## APPENDIX B

Volume 120, number 4,5

CHEMICAL PHYSICS LETTERS

18 October 1985

### MULTIPHOTON IONIZATION SPECTROSCOPY OF ATOMIC FLUORINE

William K. BISCHEL and Leonard E. JUSINSKI

*Chemical Physics Laboratory, SRI International, Menlo Park, CA 94025, USA*

Received 26 August 1985

The first observation of resonantly enhanced multiphoton ionization (REMPI) of atomic fluorine is reported. Four excited states are observed in the region of  $105000 \text{ cm}^{-1}$  corresponding to the  $^2\text{P}_{1/2,3/2} \rightarrow ^2\text{P}_{1/2,3/2}$  three-photon transition in a 3 + 2-photon ionization process. REMPI spectra of  $\text{F}_2$  in a 3 + 1-photon process is also observed. The resonant excited states in the spectra have been identified as the  $\text{H}^1\Sigma_u$  and  $\text{h}^3\Sigma_{1,u}$  levels using absorption spectra. We estimate an F-atom detection sensitivity for the present experiment of  $\approx 10^{12} \text{ cm}^{-3}$ .

#### 1. Introduction

The study of the electronic spectrum of atomic fluorine is extremely difficult since all the single-photon transitions from the ground state require wavelengths that are below the LIF window cutoff at 106 nm. The resonance transition occurs at 95.5 nm, and all other allowed absorption transitions are at shorter wavelengths. Because of the inaccessibility of these electronic states, there have been few experiments reporting the detection and spectroscopy of atomic fluorine [1,2]. This situation presents an ideal application for the techniques of multiphoton excitation, followed by either fluorescence or ionization detection.

We report here the first observation of resonantly enhanced multiphoton ionization (REMPI) of atomic fluorine in a 3 + 2-photon process. The excited states that are three-photon resonant in this experiment are the  $^2\text{P}_{3/2,1/2}$  states at  $104731.0 \text{ cm}^{-1}$  and  $105056.3 \text{ cm}^{-1}$ , respectively [3] and are illustrated in fig. 1. These states are then ionized by the absorption of two additional photons forming a five-photon (3 + 2) process. Since the ground-state fine-structure splitting between the  $^2\text{P}_{3/2,1/2}$  states is  $404.1 \text{ cm}^{-1}$  (3/2 lower), we expect that the REMPI spectrum would have four transitions if both these states were populated (observation of the hyperfine structure [2] is below our resolution limit). Thus the observation of these four transitions would form unambiguous evidence that atomic fluorine has been detected using REMPI. The

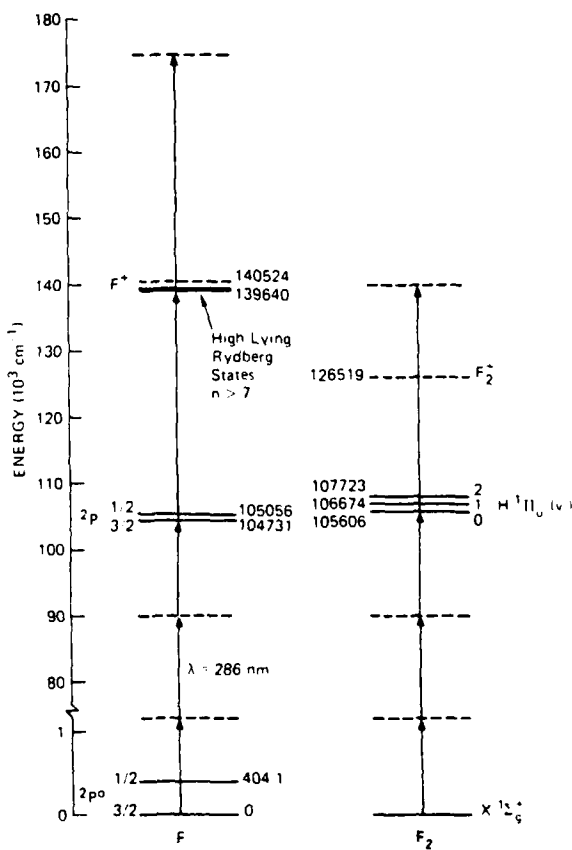


Fig. 1. Energy levels of F and  $\text{F}_2$  involved in the REMPI spectrum shown in fig. 2.

four transition wavelengths correspond to vacuum dye laser wavelengths of: 287.56 nm ( $1/2 \rightarrow 3/2$ ), 286.67 nm ( $1/2 \rightarrow 1/2$ ), 286.45 nm ( $3/2 \rightarrow 3/2$ ), and 285.56 nm ( $3/2 \rightarrow 1/2$ ).

Since the ionization limit [3] occurs at  $140524.5 \text{ cm}^{-1}$ , the possibility of  $4 + 1$  REMPI process also exists as is illustrated in fig. 1. Starting from the  $2\text{P}_{3/2}$  ground state, the equivalent energy of four UV laser photons accesses excited states in the  $2\text{S}_1^0$ ,  $2\text{P}_1^0$ ,  $2\text{D}_3^0$  manifolds that are  $\approx 880 \text{ cm}^{-1}$  below the ionization limit. These states could also be observed if there were near coincidences with the wavelengths for the three-photon resonant states. We give evidence below that we also observe these states in our REMPI experiments.

## 2. Experimental

The experimental apparatus is relatively simple. The laser photons at 285 nm are produced by doubling a Quanta Ray YAG-pumped dye laser giving a maximum UV energy of approximately 15–20 mJ. This energy is varied to obtain approximate power dependences of the ion yields by turning an achromatic half-wave plate before the doubler crystal. This allows us to change laser intensity in the cell without changing the beam quality or divergence.

The UV laser was initially focused into the experimental cell with a 20 cm focal length suprasil lens. The laser energy was measured after the cell with a calorimeter, and the temporal pulse shape was measured (fwhm of 5.5 ns) using a fast photodiode and Tek 7104 oscilloscope. The spatial profile of the laser beam at the focus was measured by scanning a  $10 \mu\text{m}$  diameter pinhole through the laser beam. For the 20 cm focusing lens, the maximum peak intensity used in this experiment was  $\approx 5 \times 10^{11} \text{ W/cm}^2$ . The intensity was reduced to  $\approx 10^9 \text{ W/cm}^2$  later in the experiment to obtain high-resolution spectra.

The cell is constructed of pyrex with suprasil Brewster windows. In the cell are two electrodes biased at +90 V. The negative electrode collects the positive ions produced in the focal volume of the laser and is grounded through an Ortec 142PC charge amplifier. The resulting signal is recorded using a boxcar averager and strip chart recorder. We estimate that it is necessary to produce approximately  $10^4$  ions per laser pulse in the focal volume to achieve a 1:1 signal to background ratio.

We flow a mixture of 10%  $\text{F}_2$  in He into the cell at a slow rate to prevent  $\text{F}_2$  loss to the pyrex walls of the cell. There is an activated charcoal  $\text{F}_2$  filter between the roughing pump and the cell. All data presented here were taken with a total pressure of 1 Torr (0.1 Torr  $\text{F}_2$ ) as measured with a 10 Torr Baraton capacitive manometer.

The F atoms are produced by UV photolysis of  $\text{F}_2$  at 286 nm, using the same laser used to excite the multiphoton transition. The absorption cross section for the transition  $\text{F}_2 + h\nu \rightarrow 2\text{F}$  peaks at approximately 280 nm with a value of approximately  $2 \times 10^{-20} \text{ cm}^2$  [4]. We estimate that the  $\text{F}_2$  is completely dissociated at the highest intensities used in our experiment while only  $\approx 15\%$  is dissociated at  $10^9 \text{ W/cm}^2$ . However, we note here that REMPI signals from  $\text{F}_2$  were observed at all intensities, resulting from ionization in the wings of the spatial profile of the laser.

## 3. Results and discussion

The MPI spectrum for a low-resolution scan of the UV laser from 291 to 278 nm (equivalent three-photon energy of  $103000$ – $108000 \text{ cm}^{-1}$ ) is given by the solid line in fig. 2 for tight focusing conditions ( $f = 20 \text{ cm}$ ). The laser energy is given by the dashed line. There are three prominent resonances in this spectrum that correspond to the above three-photon resonant transitions in F, thus confirming that F atoms are being observed. The fourth transition, barely observable in this spectrum, is obscured by background signals. These transi-

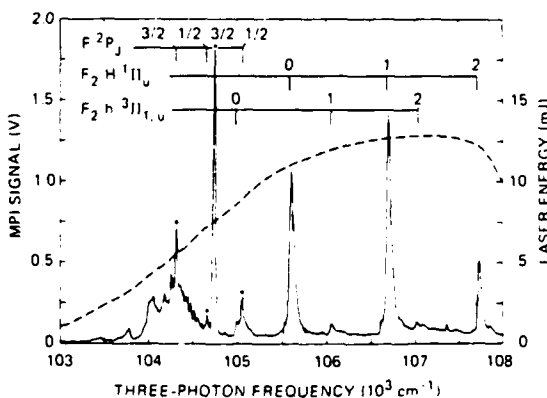


Fig. 2. Low-resolution REMPI spectrum of F and  $\text{F}_2$ . The dashed line is the laser energy.

tions are labeled in the figure by the  $J$  of the excited  $^2P$  state. If the peak laser energy is reduced from 13 mJ to 3.5 mJ, the F-atom REMPI signals disappear completely from the spectrum while the  $F_2$  signals are reduced by only a factor of 15. This is additional evidence that we have properly identified the four transitions in fig. 2 as F-atom signals.

Note in fig. 1 that the F-atom transition  $^2P_{3/2}^0 \rightarrow ^2P_{3/2}$  at  $104731\text{ cm}^{-1}$  is more than five times larger than any of the other atomic transitions. This effect is much larger than can be explained by differences in three-photon line strength factors and relative ground-state populations. We interpret this enhancement as due to accidental resonances with Rydberg states near the ionization limit, thus making the REMPI signal a  $3 + 1 + 1$ -photon process instead of a  $3 + 2$ -process. The intensity dependence of this transition is discussed below.

The other features observed and labeled in the spectrum given in fig. 2 correspond to transitions to the H  $^1\Pi_u$ , and the h  $^3\Pi_{1,u}$  states in  $F_2$  that have previously been observed in single photon absorption [5]. An analysis of these transitions will be given in a subsequent paper.

The broad feature in the region of  $104000\text{ cm}^{-1}$  has been identified [6–8] as a background signal from  $2 + 1$  photoionization of  $O_2$  (resonant state is the  $^3\Pi_g(v' = 2)$ ) by putting pure  $O_2$  into the cell and taking a REMPI spectrum. In the same manner, we also tested for background signals from the REMPI of  $N_2$  [9]. None of the features in fig. 2 could be assigned to the transitions observed in  $N_2$ . All the transitions in fig. 2 are severely broadened due to the ac Stark effect. The laser intensity had to be reduced in order to increase the resolution and accurately measure the intensity dependence of the signal.

To achieve this, the spatial profile of the laser intensity was defined by inserting a spatial filter before the cell and imaging the pinhole ( $300\text{ }\mu\text{m}$  diameter) into the cell with a 2:1 lens system. The intensity distribution in the focal volume was measured to be circularly symmetric by scanning a pinhole through the beam at different points along the propagation axis. At the focus the fwhm beam diameter was  $0.017\text{ cm}$  with a Rayleigh range of approximately  $1.8\text{ cm}$ . Assuming a Gaussian form for the spatial profile, the peak laser intensity was  $800\text{ MW/cm}^2$  for every mJ of measured laser energy.

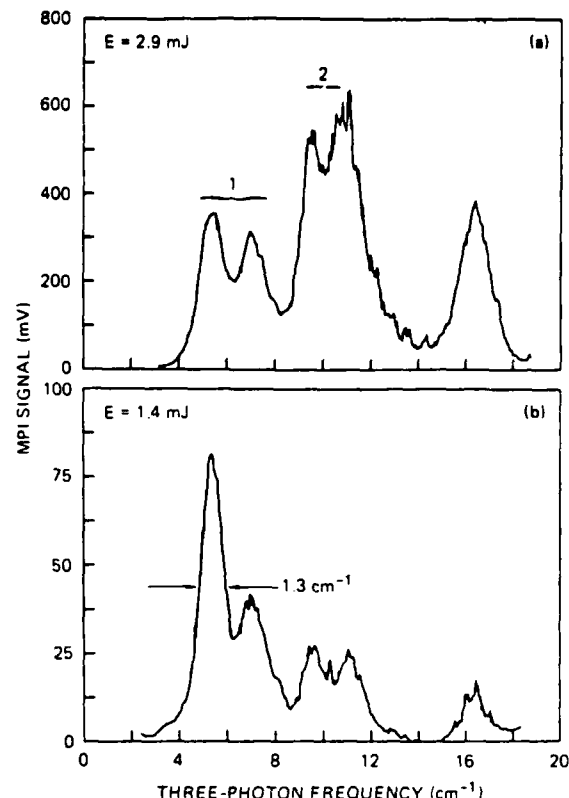


Fig. 3. High-resolution scan of the  $^2P_{3/2}^0 \rightarrow ^2P_{3/2}$  transition at  $104731\text{ cm}^{-1}$  for two different laser energies.

With the intensity reduced, we have taken high-resolution scans of the strong feature at  $104731\text{ cm}^{-1}$  identified as the  $^2P_{3/2}^0 \rightarrow ^2P_{3/2}$  three-photon resonant transition in F. These data are given in fig. 3 for two different laser energies. Note from fig. 3b that the resolution is approximately  $1.3\text{ cm}^{-1}$  limited by the linewidth of the fundamental dye laser ( $\approx 0.25\text{ cm}^{-1}$ ). We observe five different peaks (instead of one). We interpret this observation as a combination of the  $3 + 2$  and  $4 + 1$  (near  $3 + 1 + 1$ ) ionization processes discussed above. In addition, the ion signals labeled by 1 and 2 in fig. 3a have a different dependence on the laser intensity. Given our REMPI signals, we were able to vary the laser intensity from 800 to  $2400\text{ MW/cm}^2$  (laser energy of 1–3 mJ). Over this limited range, the order  $n$  intensity dependence of feature 1 is  $n = 2.6$  while the order for feature 2 is  $n = 5.0$ . If we could have obtained signals at low enough intensity, the

order of the process would have been between 5 and 6, depending on how much of the  $F_2$  has been dissociated in the experiment.

The intensity dependence of MPI transitions is difficult to accurately measure and interpret, even for non-resonant processes [9,10]. In addition to the shot-to-shot changes in the laser beam profile (both temporal and spatial) that plague all MPI experiments [10], the intensity dependence of the REMPI signals in this experiment are complicated by two other factors. First, the single-photon resonant steps in the  $3 + 2$  (near  $3 + 1 + 1$ ) processes may be saturated at these intensities, thus reducing the order of the observed intensity dependence. In addition, the ac Stark effect can shift levels into (or out of) resonance [11], thereby changing the apparent order of the intensity dependence. However, we can detect no change in the position of the peaks of the transitions given in fig. 3 at the different laser intensities. Thus, we conclude that only saturation plays a significant role in determining the order for the intensity dependence of the data in fig. 3.

Second, the ground-state F-atom density is varying during the laser pulse and thus the order of the intensity dependence will reflect the degree of dissociation of  $F_2$ . Both of these effects make the modelling of the ionization process unproductive without data over a much larger intensity range (several orders of magnitude). If such data were available, effective cross sections for each step of the ionization process could, in principle, be determined by fitting the entire intensity dependence of the ionization yield curve as has been done in the case of the  $3 + 1$  REMPI of xenon [12]. Experiments of this type are necessary if REMPI is ever to be used to measure absolute F-atom concentrations for an arbitrary laser intensity.

We can, however, make estimates of the F-atom detection sensitivity in the present experiment. The slope of the ion yield curve for feature 2 in fig. 3a is  $6.0 \text{ mV/mJ}$  [5]. At  $3 \text{ mJ}$  of laser energy, we estimate that we have a ground-state density at the time of peak laser intensity of approximately  $10^{15} \text{ F atoms/cm}^3$ . For this density, we can obtain a signal/background ratio of greater than  $1000:1$ , giving a F-atom detection sensitivity of approximately  $10^{12} \text{ cm}^{-3}$ . This is unoptimized with respect to a number of parameters and thus could be significantly improved. Since  $1 \text{ mV}$  of signal corresponds to approximately

$5 \times 10^3$  ions, the signal in fig. 3b corresponds to  $\approx 4 \times 10^5$  ions. In this experiment, the excitation volume is  $\approx 2 \times 10^{-4} \text{ cm}^{-3}$  and thus approximately  $\approx 2 \times 10^{-6}$  of the ground-state F-atoms have been ionized.

We plan to modify the apparatus to include time-of-flight mass analysis of the ion signal to eliminate background signals from  $F_2$  and  $O_2$  and enhance the detection sensitivity. This should allow two-color experiments to study the odd parity Rydberg states near the ionization limit. In addition, the enhanced detection sensitivity will allow the intensity dependence of the ionization yield to be determined over a much larger range. And finally, we plan to look for third and fifth harmonic radiation at 95 and 57 nm which should compete with the ionization process at higher F-atom densities [13].

#### 4. Conclusion

In conclusion, we have unambiguously demonstrated for the first time the detection of atomic fluorine using REMPI with a sensitivity limit of approximately  $10^{12} \text{ cm}^{-3}$  for the present experimental arrangement. This limit can probably be reduced by several orders of magnitude in a two-color experiment. We anticipate that these results can be utilized in a number of research areas requiring the sensitive detection of spatially and temporally resolved F-atom distributions.

#### Acknowledgement

This work was supported by AFOSR under Contract No. F4620-85-K-0005.

#### References

- [1] M.A.A. Clyne and W.S. Nip, *J. Chem. Soc. Faraday Trans. II* 73 (1977) 1308.
- [2] A.C. Stanton and C.E. Kolb, *J. Chem. Phys.* 72 (1980) 6637.
- [3] S. Bashkin and J.A. Stoner Jr., *Atomic energy levels and Grotrian diagrams*, Vol. 1 (North-Holland, Amsterdam, 1975) p. 165.
- [4] R.K. Steunenberg and R.C. Vogel, *J. Am. Chem. Soc.* 78 (1956) 901.

- [5] E.A. Colbourn, M. Dagenais, A.E. Douglas and J.W. Raymonda, *Can. J. Phys.* 54 (1976) 1343.
- [6] A. Sur, C.V. Ramana and S.D. Colson, *J. Chem. Phys.* 83 (1985) 904.
- [7] R.P. Saxon and B. Liu, *J. Chem. Phys.* 73 (1980) 870.
- [8] P.L. Houston, private communication.
- [9] S.T. Pratt, P.M. Dehmer and J.L. Dehmer, *J. Chem. Phys.* 81 (1985) 3444.
- [10] J. Morellec, D. Normand and G. Petite, in: *Advances in atomic and molecular physics*, Vol. 18, eds. Sir David Bates and B. Bederson (Academic Press, New York, 1982) p. 97.
- [11] L. Allen, R.W. Boyd, J. Krasinski, M.S. Malcuit and C.R. Stroud, *Phys. Rev. Letters* 54 (1985) 309.
- [12] M.G. Payne, C.H. Payne, G.S. Hurst and G.W. Foltz, in: *Advances in atomic and molecular physics*, Vol. 17, eds. Sir David Bates and B. Bederson (Academic Press, New York, 1981) pp. 229-274.
- [13] D.J. Jackson and J.J. Wynne, *Phys. Rev. Letters* 49 (1982) 543.

APPENDIX C

MECHANISMS FOR  $F^+$  PRODUCTION IN THE MULTIPHOTON IONIZATION OF  $F_2$

APPENDIX C

MECHANISMS FOR F<sup>+</sup> PRODUCTION IN THE  
MULTIPHOTON IONIZATION OF F<sub>2</sub>

G. C. Herring, Leonard E. Jusinski, Mark J. Dyer, and  
William K. Bischel  
SRI International, Chemical Physics Laboratory  
333 Ravenswood Avenue,  
Menlo Park, CA 94025

ABSTRACT

Resonantly-enhanced multiphoton ionization (REMPI) spectra of F and F<sub>2</sub> have been obtained using a 285 nm laser and a time-of-flight mass spectrometer. We observe that 3 + 1 REMPI of F<sub>2</sub> produces only F<sup>+</sup> and no detectable F<sub>2</sub><sup>+</sup>. Possible mechanisms for this F<sup>+</sup> production are discussed, including a comparison to similar studies in H<sub>2</sub>.

Prepared for submission to: Rapid Communications, Physical Review A

MP 87-196  
July 20, 1987

## INTRODUCTION

A recent study<sup>1</sup> of the resonantly enhanced multiphoton ionization (REMPI) of F and F<sub>2</sub> was performed in a bulb experiment where the total ion current was observed. Since 285 nm can readily photodissociate F<sub>2</sub>, spectral features from both F and F<sub>2</sub> were observed from a F<sub>2</sub> sample while a laser was tuned through the 285 nm region. This combined F/F<sub>2</sub> spectrum and additional lines from impurities (O<sub>2</sub>) made it difficult to clearly interpret some of the data from this experiment. Thus we built a time-of-flight (TOF) mass spectrometer to separate the various ionic species and allow the separation of the F and F<sub>2</sub> spectra. We report the results of this experiment in the present letter.

We have measured the relative amounts of F<sup>+</sup> and F<sub>2</sub><sup>+</sup> production when the H <sup>1</sup>Π<sub>u</sub> state of F<sub>2</sub> is used as an intermediate state in a 3 + 1 REMPI process. The F<sup>+</sup> production is  $\geq 100$  times the F<sub>2</sub><sup>+</sup> production for our experimental conditions. We have also measured the kinetic energy release of the positive ions associated with this process and found a value consistent with the known dissociation energy of F<sub>2</sub><sup>+</sup>. These results imply that we are first producing F<sub>2</sub><sup>+</sup> that is subsequently photodissociated. However, this scenario is not the only one that is consistent with our data. For example, the dissociation of H<sub>2</sub> to produce neutral F atoms that are then ionized via a single-photon absorption is also consistent with our results. Thus the purpose of this paper is to discuss the possible mechanisms that may contribute to the F<sup>+</sup> production that we observe.

This F<sup>+</sup> production during the REMPI of F<sub>2</sub> is very similar to H<sup>+</sup> production during the REMPI of H<sub>2</sub>. Currently, there is much discussion in the literature about H<sup>+</sup> production either by the dissociation of H<sub>2</sub><sup>+</sup> or by the dissociation of H<sub>2</sub> followed by the ionization of excited atomic H. H<sup>+</sup> production has recently been reported<sup>2-4</sup> and is now under investigation by several groups.<sup>5-9</sup> The competition of dissociation and ionization in NO has also recently been studied.<sup>10</sup> The present observation of F<sup>+</sup> production further illustrates the importance of the competition between dissociation and ionization for a variety of diatomic molecules.

## EXPERIMENTAL

Tunable 285 nm light is produced by frequency doubling a Quanta Ray YAG-pumped PDL-1 dye laser. Typically, about 10 to 15 mJ/pulse of UV with a 0.5 cm<sup>-1</sup> bandwidth are delivered to the ionization region at a 10 Hz repetition rate. The beam is focused into the ionization region with a 25 cm lens that gives a peak intensity on the order of 10<sup>12</sup> W cm<sup>-2</sup>.

A pulsed molecular F<sub>2</sub> source was produced using a pulsed valve with the ionization region located about 1 cm downstream from the nozzle aperture (100 μm diameter). We used commercially available He/F<sub>2</sub> mixtures (5% F<sub>2</sub>) that typically contained a few percent of O<sub>2</sub> impurities. With gas pulse widths of 300 μs, we could keep 4500 Torr behind the nozzle while maintaining the background vacuum surrounding the ionization region and the flight path of the TOF spectrometer at 3 × 10<sup>-5</sup> Torr. The density of F<sub>2</sub> in the ionization region was about 10<sup>14</sup> cm<sup>-3</sup>.

The TOF mass spectrometer is built following the design of Wiley and McLaren.<sup>11</sup> After photoionization, the positive ions are extracted along an axis perpendicular to the laser beam and accelerated toward an electron multiplier with BeCu dynodes. Both the ionization and acceleration regions of the TOF spectrometer are 1 cm long, while the field-free flight region is about 20 cm long. We typically use 300 V across the ionization region, 400 V across the acceleration region, a grounded 20 cm flight path, and 3000 V across the electron multiplier. All of these voltages are dc. These parameters give a total flight time of 3 μs, 50 ns (FWHM) pulse widths, and single mass resolution for masses of 20 amu.

The entire mass spectrum is monitored with an oscilloscope, and species of interest are monitored with boxcar integrators. This arrangement allows the simultaneous recording of two or more mass signals during a single laser scan. Time constants are normally about 1-3 s.

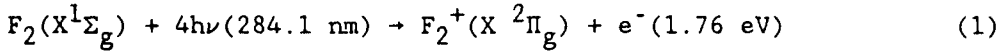
## RESULTS AND DISCUSSION

### 3 + 1 + 1 Dissociation/Ionization of F<sub>2</sub>

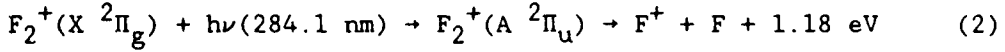
The primary result of this research is the finding that 3+1 REMPI [resonant state is H  $^1\Pi(v = 0)$ ] in F<sub>2</sub> surprisingly produces F<sup>+</sup> rather than F<sub>2</sub><sup>+</sup>. This finding is based on the fact that our TOF spectra show a strong F<sup>+</sup> signal and no observable F<sub>2</sub><sup>+</sup> ions when the laser is tuned over the known F<sub>2</sub> resonance at 284.1 nm. We did not observe any F<sub>2</sub><sup>+</sup> under any conditions, including reduced laser powers. Our best signal-to-noise ratio for F<sup>+</sup> was about 10<sup>2</sup>, so the F<sub>2</sub><sup>+</sup> production was at least 10<sup>2</sup> times smaller than the F<sup>+</sup> production. In this section we will discuss three of the mechanisms most likely responsible for producing the F<sup>+</sup>.

A typical TOF spectra, with the laser tuned to the F<sub>2</sub> resonance at 284.1 nm, is shown in Figure 1. The low resolution trace in the top of Figure 1 shows a strong F<sup>+</sup> signal and the absence of any F<sub>2</sub><sup>+</sup> when the laser is linearly polarized with the electric field perpendicular to the TOF axis. The high resolution traces in the bottom of Figure 1 show the time profile of the F<sup>+</sup> ion pulse for two different laser polarizations. The single peak appears when the laser electric field of the laser is perpendicular to the TOF axis (same condition as the upper trace) and the double peak appears when the electric field is parallel to the TOF axis. The reason for these two different profiles of the F<sup>+</sup> peak is discussed in more detail below.

The first possible mechanism (1) for F<sup>+</sup> production is a two-step process consisting of



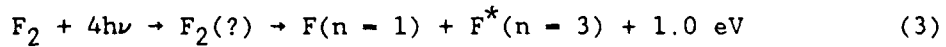
and



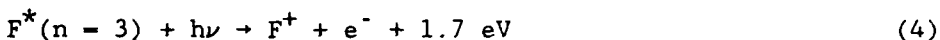
where the 1.18 eV kinetic energy release represents the total kinetic energy of the dissociation fragments. Since the  $^1\Pi_u$   $F_2$  state is a Rydberg state, its potential curve will closely follow the  $F_2^+$  ground state curve and the  $v = 0 \rightarrow 0$  Frank-Condon factor should dominate during the ionization process. In determining the kinetic energy release of Equation 2 we have assumed that the  $F_2^+ X$  state is formed with  $v = 0$  and have used the value of the  $F_2^+$  ground state dissociation energy of Reference 12. The process of Equations 1 and 2 is illustrated by the five upward arrows (representing absorbed photons) and the wavy downward arrow (representing the 1.76 eV photoelectron) shown in the left hand side of Figure 2.

We have tested the hypothesis of Equations 1 and 2 by measuring the kinetic energy release associated with our signal. This measurement is possible because the TOF ion signal at the  $F^+$  mass exhibits a double-peaked structure resulting from the forward/backward translational energy release in the photodissociation process. When the laser is tuned to the 284.1 nm transition in  $F_2$ , the double-peaked structure is evident when the laser polarization is parallel to the TOF detection axis. This fact indicates that the photodissociation associated with this signal occurs via a parallel transition.<sup>13</sup> The  $^2\Pi_g$  to  $^2\Pi_u$  transition in  $F_2^+$  (See Equation 2) is such a parallel transition. In contrast, the ion signal at  $F^+$  shows a single-peak structure when the laser polarization is perpendicular to the TOF collection axis. Time profiles for the  $F^+$  ion signal for both parallel and perpendicular laser polarizations are shown in the lower portion of Figure 1 for the  $F_2$  resonance at 284.1 nm. The peak separation of the double-peak structure is related to the TOF spectrometer dimensions and voltages as given in Reference 11. We have measured the peak separation as a function of ionization voltage and determined that the kinetic energy release is  $1.0 \pm 0.1$  ev, consistent with the energy release shown in Equation 2. Thus the mechanism of Equations 1 and 2 is in agreement with our measurement.

A second possible mechanism (2) for producing  $F^+$  is also a two-step process. The process is given by



and



This process is also shown in Figure 2. The four lowest upward arrows on the left side of the figure are the four absorbed photons in Equation 3, and the unbound dotted potential curve represents the unknown dissociating state. The single-photon ionization of the excited atom in Equation 4 is shown with the two arrows on the right side of the figure.

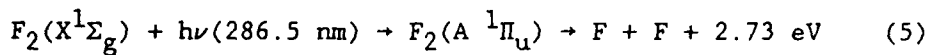
Although the existence of unbound states of the neutral  $F_2$  molecule that lie above the ionization limit has not been reported in the literature, we assume their existence in  $F_2$  because similar states are well known in  $H_2$ . Recently, Chupka<sup>7</sup> and Hickman<sup>8</sup> have used these states to make quantitative predictions of the relative amounts of  $H^+$  and  $H_2^+$  during photoexcitation. Xu et al.<sup>5</sup> have experimentally confirmed these theoretical results. Thus, the importance of mechanism 2 has been proved in  $H_2$  and must be considered a potential source for  $F^+$  production from  $F_2$ . Since both mechanisms (1) and 2 predict energy releases within 10% of our measured value, the present experiment cannot reveal the relative contributions to the  $F^+$  production. However, the different kinetic energies of the photoelectrons for the two mechanisms would permit any experiment that measures electron energies to establish the relative contributions.

A third possible mechanism (3) for the  $F^+$  production that we observe is the dissociation process that leads to the  $F^+, F^-$  ion pair. However, we can rule out this mechanism because the asymptotes of the intermediate states of this process are well known<sup>14</sup> and their values preclude the energy release of 1.0 ev that we measure.

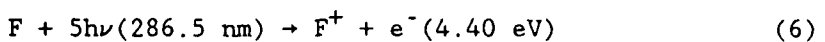
### 3 + 2 REMPI of Atomic Fluorine

When the laser is tuned to the 3 + 2 REMPI transition in atomic fluorine at 286.5 nm (resonant state is  $^2P_{3/2}$ ), we again observe only  $F^+$  ions, as expected. In this case, the double-peak structure is observed when the laser

polarization is perpendicular to the TOF detection axis and the single peak appears when the polarization is parallel to the TOF detection axis. This result indicates that the photodissociation of our signal occurs by a perpendicular transition. If the mechanism for  $F^+$  production is assumed to be a two step process of



and



then the  $^1\Sigma_g$  to  $^1\Pi_u$  perpendicular transition of Equation 3 is consistent with our data. We have used the well-known dissociation energy<sup>14-16</sup> of  $F_2$  to arrive at the kinetic energy release of Equation 5. We have also measured this energy release to be  $3.0 \pm 0.3$  ev by using the same method as described above for the  $3 + 1 + 1$  REMPI/dissociation process discussed above. The good agreement of this measurement and Equation 5 indicates that the 1.0 ev measurement in the previous section is accurate to 10%.

#### SUMMARY

Photoionization of atomic and molecular fluorine in the 285 nm region has been studied with a TOF mass spectrometer. When the laser is three-photon resonant with the  $H^1\Pi_u$  ( $v = 0$ ) state in  $F_2$ , we find that there is a strongly favored mechanism that produces  $F^+$  instead of  $F_2^+$ . The two most likely mechanisms are (1) the ionization of  $F_2$  followed by the immediate dissociation of  $F_2^+$  and (2) the dissociation of  $F_2$  into one ground state and one excited state atom followed by the ionization of the excited fluorine atom. We are unable to specify the relative contribution of these two mechanisms from the present measurements of dissociation fragment energies. Thus future work in this area should include electron energy measurements that would unambiguously show the relative contribution of these two mechanisms to  $F^+$  formation.

#### ACKNOWLEDGEMENTS

This work was supported by the Air Force Office of Scientific Research under contract No. F49620-85-K-0005. G. C. Herring thanks K. T. Gillen and A. P. Hickman for helpful discussions.

## REFERENCES

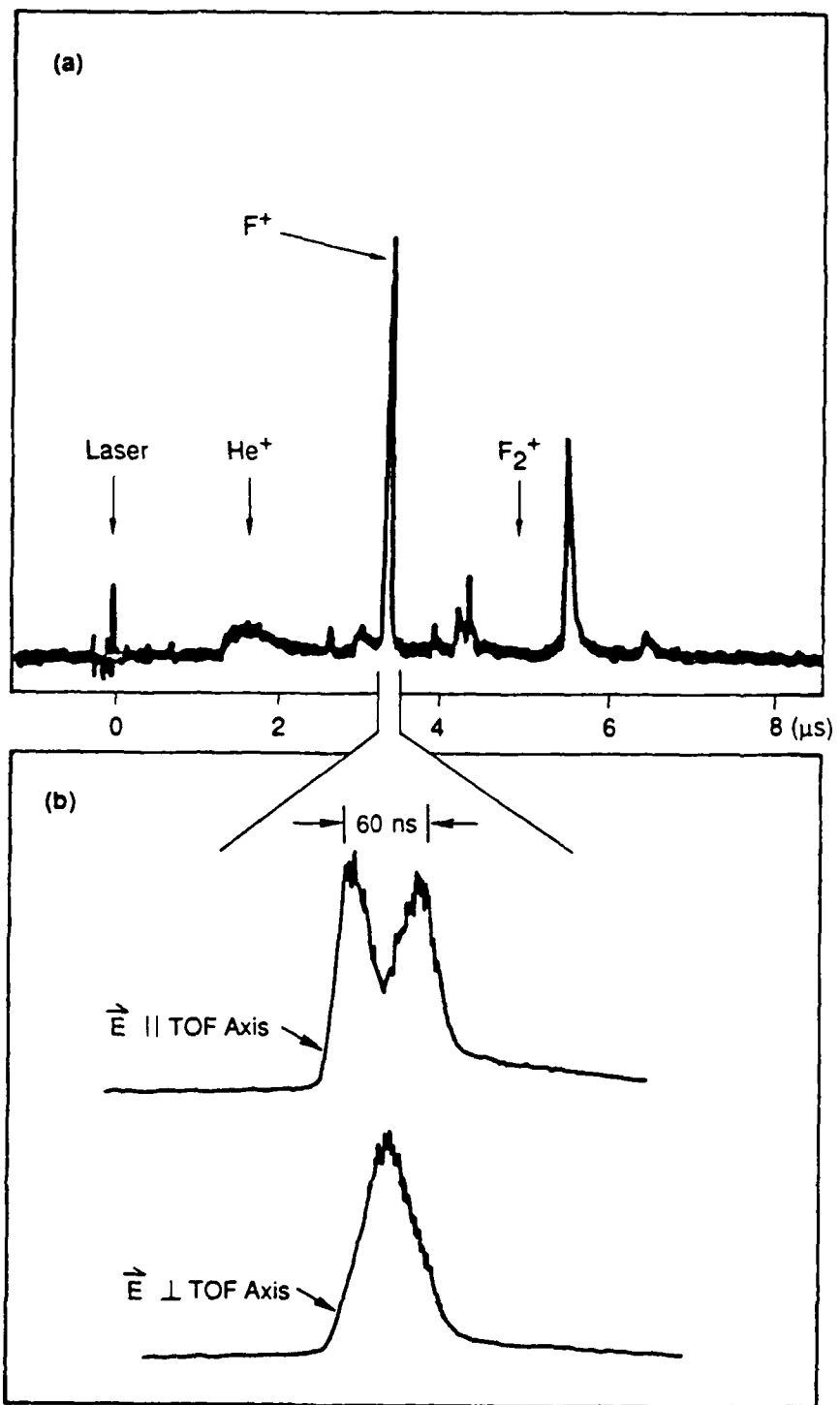
1. W. K. Bischel and L. E. Jusinski, Chem. Phys. Lett. 120, 337 (1985).
2. C. Cornaggia, J. Morellec, and D. Normand, J. Phys. B 18, L501 (1985).
3. J.H.M. Bonnie, P. J. Enshuistra, J. Los, and H. J. Hopman, Chem. Phys. Lett. 125, 27 (1986).
4. J.H.M. Bonnie, J.W.J. Verschuur, H. J. Hopman, and H. B. Van Linden Van Den Heuvell, Chem. Phys. Lett. 130, 43 (1986).
5. E. Xu, Tsuboi, R. Kachru, and H. Helm, "Four Photon Dissociation and Ionization of H<sub>2</sub>," to be published (1987)
6. J. D. Buck, D. H. Parker, D. W. Chandler, "Proton Production in Double Resonant Laser Excitation," to be published (1987)
7. W. A. Chupka, J. Chem. Phys. 86, in press (1987).
8. A. P. Hickman, "Non Frank-Condon Distribution of Final States in Photoionization of H<sub>2</sub> (C <sup>1</sup>Π<sub>u</sub>)," submitted to Phys. Rev. Lett. (1987).
9. M. A. O'Halloran, S. T. Pratt, P. M. Dehmer, and J. L. Dehmer, "Photoionization Dynamics of H<sub>2</sub>C<sup>1</sup>Π<sub>u</sub>: Vibrational and Rotational Branching Ratios," submitted to J. Chem. Phys. (1987).
10. A. Giusti-Suzor and Ch. Jung, J. Chem. Phys. 80, 986 (1984).
11. W. C. Wiley and I. H. McLaren, Rev. Sci. Instr. 26, 1150 (1955).
12. J. T. Herron and V. H. Dibeler, J. Chem. Phys. 32, 1884 (1960).
13. Richard N. Zare, Thesis, Harvard University (1964).

14. E. A. Colbourn, M. Dagenais, A. E. Douglas, and J. W. Raymonda, Can. J. Phys. 54, 1343 (1976).
15. J. Berkowitz, W. A. Chupka, P. M. Guyon, J. H. Holloway, and R. Spohr, J. Chem. Phys. 54, 5165 (1971).
16. J. G. Stamper and R. F. Barrow, Trans. Faraday Soc. 54, 1952 (1958).

#### FIGURE CAPTIONS

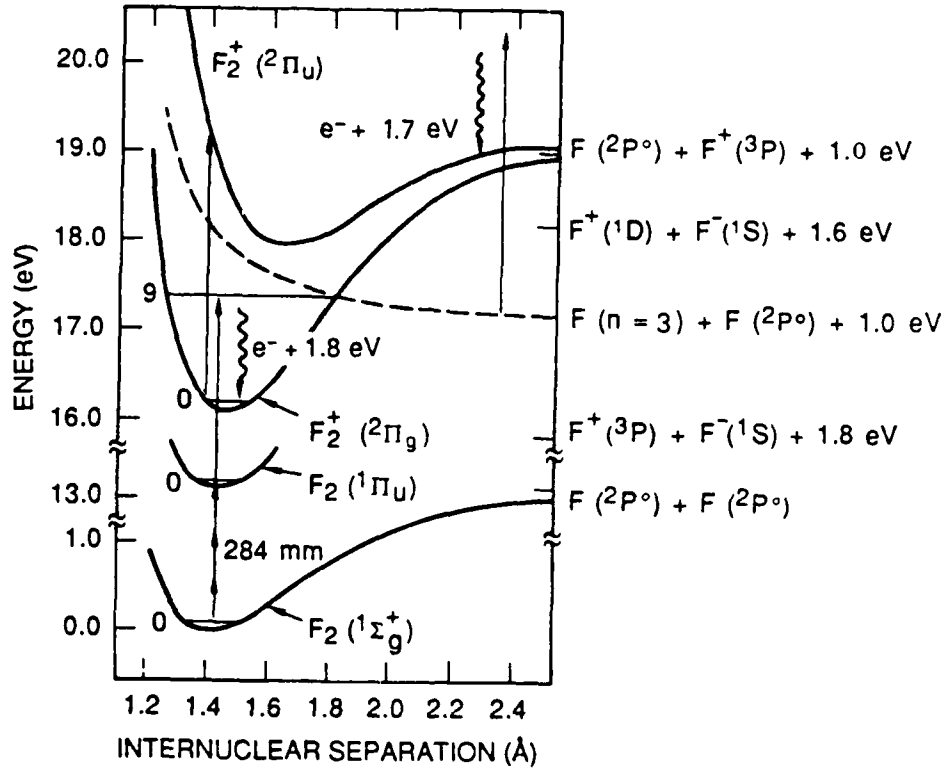
Figure 1. (a) Typical time-of-flight spectra obtained when the laser is tuned to the  $H^1\Pi_u \leftarrow X^1\Sigma_g$  transition. (b) Time profiles of the  $F^+$  signal for laser polarizations parallel and perpendicular to the time-of-flight axis.

Figure 2. Two mechanisms for  $F_2^+$  production from  $F_2$ . The six arrows on the left side illustrate mechanism (1) while the four lowermost upward arrows on the left and the two arrows on the right side illustrate mechanism (2). Solid upward arrows represent absorbed photons and wavy downward arrows represent emitted photoelectrons.



JA-m-8320-10

FIGURE 1



JA-8320-11

FIGURE 2